COMPARISON OF CIRCUIT CONFIGURATION AND FILTERING PERFORMANCE BETWEEN PARALLEL AND SERIES HYBRID ACTIVE FILTER

Leopold HERMAN
Faculty of Electrical Engineering,
University of Ljubljana – Slovenia
leopold.herman@fe.uni-lj.si

Boštjan BLAŽIČ
Faculty of Electrical Engineering,
University of Ljubljana – Slovenia
bostjan.blazic@fe.uni-lj.si

Igor PAPIČ
Faculty of Electrical Engineering,
University of Ljubljana – Slovenia
igor.papic@fe.uni-lj.si

ABSTRACT

This paper compares power ratings and filtering performance of two hybrid active filters. A novel parallel filter topology is presented and compared with most commonly used series hybrid filter topology. Both filters are composed of a small-rating active part and passive LC compensator. The main objective of the passive part is to compensate reactive power, while the active part is used to improve filtering performance and damp the resonance amplifications of current harmonics. The effectiveness of both hybrid filters is compared by means of real-time digital simulations.

INTRODUCTION

Modern compensation systems play an important role in providing the appropriate parameters of the power quality. Compensators can in general be classified into passive and active, of which the later are based on power electronics. Active filters mitigate some of the disadvantages of passive filters; however, the most notable disadvantage of active filters is their high investment and operational costs. Thus, for nonlinear loads above 1MW the passive filters are still an economical solution [1, 2].

By combining passive and active filters into a single device, their individual disadvantages can be mitigated. These devices are referred to as hybrid active power filters (HAPF). The purpose of the active part of a hybrid filter is not a standalone operation, but improving operational characteristics of the passive part. This allows us to considerably reduce the necessary power ratings of the active part, which is typically up to 10 % of the rating of passive part [3].

The hybrid filter presented in this paper is composed of a three-phase voltage-source converter connected in parallel with the passive filter inductor (Fig. 1) [4-6]. The main advantage of this structure is that the voltage drop on the capacitor reduces the VSC voltage ratings, while the inductor conducts the fundamental reactive current. In this paper, the rating requirements are analysed and compared with the most commonly used series HAPF topology (Fig. 2).

To ensure a good filtering performance of the hybrid filters, a proportional-resonant (PR) current controller is used. Resonant controllers have taken on significant importance in recent years due to their high selectivity and good performance. The filtering performance of both hybrid filters is compared by means of Real-Time Digital Simulator (RTDS) [7, 8].

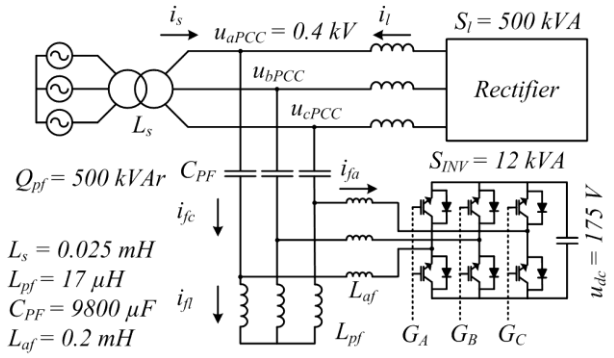

Fig. 1: Basic circuit of the parallel HAPF.

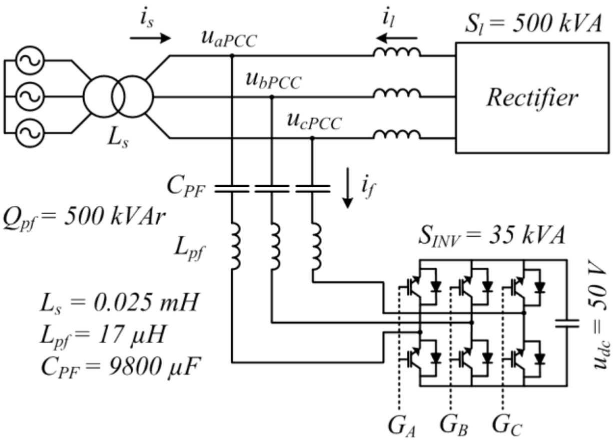

Fig. 2: Basic circuit of the series HAPF.

SYSTEM CONFIGURATION

Figure 1 shows a detailed scheme of the proposed HAPF. It consists of a three-phase two-level voltage-source converter (VSC) rated at 12 kVA and a passive part (elements L_{pf} and C_{pf}) connected in parallel. The passive part is rated at 500 kVAr and tuned to 390 Hz. The HAPF is designed to compensate the reactive power of a 500 kVA three–phase, six–pulse rectifier and to reduce the total harmonic distortion (THD) of the supply current i_s below 5 %.

The central unit of the active filter is the VSC. It is comprised of 6 IGBT semiconductor switches with anti-parallel diodes and capacitor on the dc-side. The voltage ratings and capacitor size are determined by the current harmonics to be compensated. According to the selected type of converter, the device can be described as a controllable voltage source [3].

Figure 2 shows a series HAPF topology. It consists of a three-phase two-level VSC rated at 35 kVA and a combination of inductance L_{pf} and capacitance C_{pf} connected in series. To connect the device to the network no coupling transformer is needed. The capacitor represents high impedance for the basic component of the voltage, thus most of the voltage drop occurs on the capacitor [9, 10].

Rating Analysis

The Series Hybrid Active Filter

The voltage across the active part of the hybrid filter consists of two components: component due to the distorted supply voltage ($\underline{U}_{S,h}$) and component due to the harmonic load current ($\underline{I}_{L,h}$) flowing in the passive impedance. This voltage is given by (1).

$$\begin{aligned}\underline{U}_{AF} &= \sum_{h=3,5...} (\underline{U}_{S,h} + \underline{I}_{L,h}(\underline{X}_{C,h} - \underline{X}_{L,h})) = \\ &= \sum_{h=3,5...} (\underline{U}_{S,h} + \underline{I}_{L,h}\underline{X}_{C,1}\frac{f_1}{f_h}(1-\frac{f_h^2}{f_t^2}))\end{aligned} \quad (1)$$

Here f_1 is fundamental frequency (i.e. 50 Hz), f_h is frequency of the corresponding harmonic and f_t is tuned frequency of the passive filter.

The current flowing in the active part also consists of two parts – harmonic component, due to the distorted load current and fundamental component.

$$\underline{I}_{AF,h} = \sum_{h=3,5...} (\frac{\underline{U}_{S,1}}{Z_{PF,1}} + \underline{I}_{L,h}) = \sum_{h=3,5...} (\frac{\underline{U}_{S,1}}{X_{C,1}}\frac{f_t^2}{f_t^2 - f_1^2} + \underline{I}_{L,h}) \quad (2)$$

The power rating requirements of the active part are given by (3).

$$S_{AF} = U_{AF} \cdot I_{AF} \quad (3)$$

Let us consider the following example case [11]:

$U_{S,1} = 1\angle 0$, $I_{L,1} = 1\angle\frac{\pi}{4}$, $U_{S,h} = 0$, $I_{L,5} = \frac{1}{5}I_{L,1}$,

$\varphi_{I,5} = 5\cdot\varphi_1$, $I_{L,7} = \frac{1}{7}I_{L,1}$, $\varphi_{I,7} = 7\cdot\varphi_1$, $f_t = 240Hz$.

For this case the required power of the active part is given by:

$$S_{AF} = U_{AF,rms} \cdot I_{AF,rms} = 0.025 p.u. \quad (4)$$

The Parallel Hybrid Active Filter

The active part of parallel HAPF has to provide a small component of base voltage at the point of common coupling (PCC) in order to divert the base reactive current to flow in the inductor i_{fl}. This voltage is equal to the voltage drop on the inductor for a pure passive filter and it depends on the tuned frequency of the passive part. It can be expressed as:

$$\underline{U}_{AF,1} = \underline{U}_{S,1}\frac{1}{1-\frac{f_t^2}{f_1^2}}. \quad (5)$$

The harmonic voltage across the active part is given by:

$$\underline{U}_{AF,h} = \underline{U}_{S,h} + j\cdot\underline{I}_{L,h}\cdot X_{C,h}. \quad (6)$$

To get the worst case, no load impedance was considered when deriving (6). The active filter inductance L_{af} was neglected and the harmonic current flowing in the system was considered to be zero.

The current flowing in the active part is given by:

$$\underline{I}_{AF,h} = \underline{U}_{S,h}\frac{j\cdot f_t^2}{f_h f_1 X_{C1}} + \underline{I}_{L,h}(1-\frac{f_t^2}{f_h^2}). \quad (7)$$

The required power of the active part is given by:

$$S_{AF} = U_{AF,rms} \cdot I_{AF,rms} = 0.0058 p.u. \quad (8)$$

As it can be seen, the required power rating of the active part is more than four times lower than the required power of the series HAPF topology. An extensive overview of the power-rating requirements for most common current-sing HAPF topologies can be found in [11].

CONTROL ALGORITHM

The control algorithm is essential for a proper and efficient operation of the HAPF. It can be divided into three parts:

- currents and voltages detection,
- reference currents and voltages determination and
- determination of control pulses for driving the semiconductor switches.

Reference Current and Voltages Determination

As it can be seen from Fig. 3 and Fig. 4, the inputs to the control system are measured three-phase supply currents $i_{s,abc}$. These currents are first transformed into the *dq*-reference frame (Fig. 5), with a rotating frequency synchronous to the base system frequency (ω_0). In the next step dc-component is removed with a first-order high-pass filter (HPF). After multiplying signals by a proportional-resonant controller transfer function, we get the reference voltages to be generated by the active part of the HAPF.

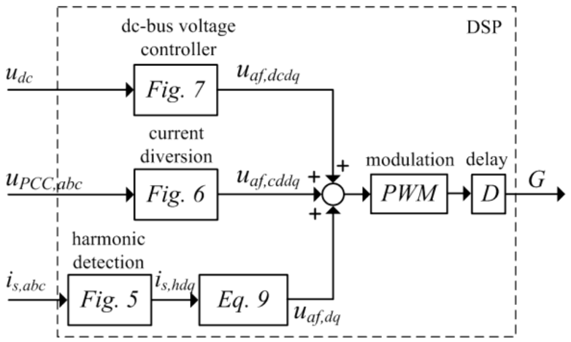

Fig. 3: Control block diagram of the parallel HAPF.

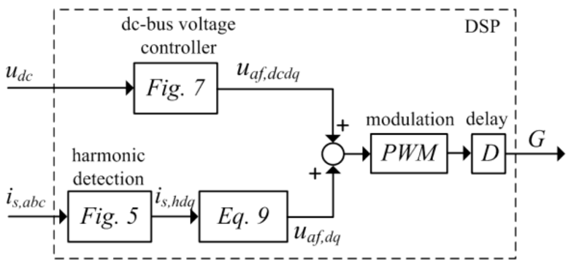

Fig. 4: Control block diagram of the series HAPF.

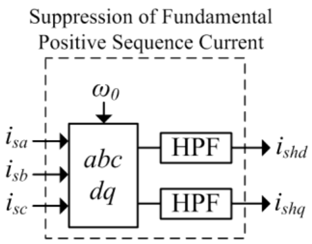

Fig. 5: Control block diagram of the harmonic current detection.

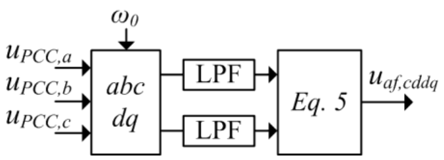

Fig. 6: Fundamental current diversion.

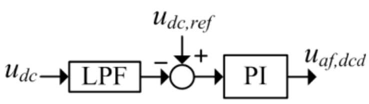

Fig. 7: DC-bus voltage control.

$$H_{PR}(s) = K_P + \sum_{h=5,7...} K_{Ih} \frac{\omega_{PR} \cdot s}{s^2 + 2\omega_{PR} \cdot s + (h \cdot \omega_1)^2} \tag{9}$$

The expression (9) can be interpreted as follows: the active part of the hybrid filter acts as a resistor of $K_P > 0$ with several resonant circuits added in series. The proportional control part K_P causes the active filter to act as an additional fictitious resistance R_{add} added in series to the system impedance Z_S that increases the damping performance of the filter. The parallel resonance gets sufficiently damped for values of $K_P > 2$.

On the other hand, by increasing the integral control part K_I high equivalent system impedances at the selected harmonic frequencies are created. If K_I is high enough, the system impedance is much higher than the filter impedance, which diverts almost all the harmonic currents injected by the nonlinear load into the filter branch.

The active part of the parallel HAPF topology (Fig. 3) has to provide a small component of base voltage at the PCC in order to divert the base reactive current to flow in the inductor. In Fig. 6 a block diagram of this current diversion is shown. Before applying Eq. 5, input signals are filtered with low-pass filter (LPF) with a cut-off frequency of 20 Hz.

DC Voltage Control

In Fig. 7 a DC-bus voltage regulator is shown. It is very important for the effective operation of the hybrid filter that the voltage on the dc side of the converter is as constant as possible. Fluctuations in the dc voltage are reflected as a voltage harmonic distortion on the ac side. The PI controller with proportional and integral gains set to 2 and 200 Ω/s is used to control the voltage.

Determination of Control Pulses to Drive the Semiconductors Switches

When the reference values are determined, the next step is to determine the control pulses to drive the semiconductor switches (IGBTs). For this purpose the pulse-width modulation (PWM) was used. The reference signals are compared to the 10 kHz carrier signal and according to the comparison switching pulses *G* are generated.

PERFORMANCE EVALUATION

The filtering performance of both hybrid filters is compared by means of Real-Time Digital Simulator (RTDS). Within the RTDS simulator a power-system model with the HAPF has been created, where the output signals correspond to the PCC voltages, system currents and the voltage at the dc-side of the inverter. These signals are fed into the Texas Instruments TMS320F28335 hardware platform as the control system. The control algorithm (Fig. 3 and 4) is implemented in the C language. The hardware produces six firing pulses that are led back to the RTDS simulator via the digital input card.

As it can be seen from the simulation results in Fig. 8 and Fig. 9, load current is highly distorted with 5th, 7th, 11th, 13th, etc., harmonics. Since the PR regulator is implemented in the rotating reference frame (*dq*-frame), only two regulators tuned at 6th and 12th harmonics are required to compensate all four. Proportional constant was set to $K_P = 2$ and both integral constants to $K_I = 550$.

The simulated waveforms of the parallel HAPF are shown

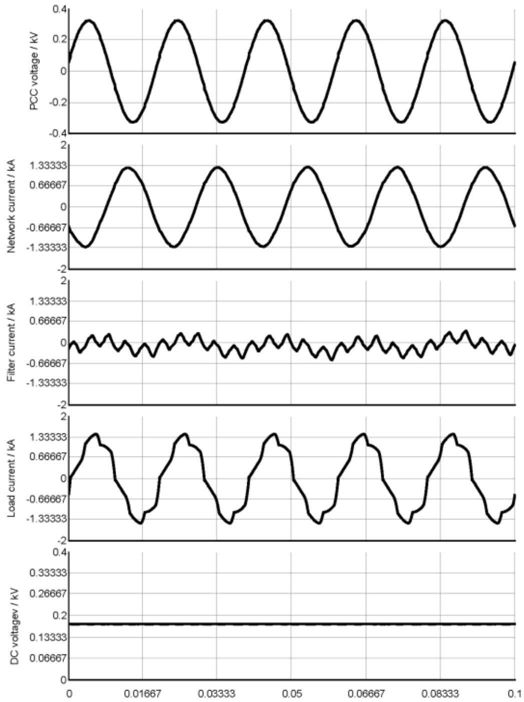

Fig. 8: Parallel HAPF simulated waveforms – voltage at HAPF PCC, supply (system) current, HAPF current, load current and voltage at the dc side of the converter.

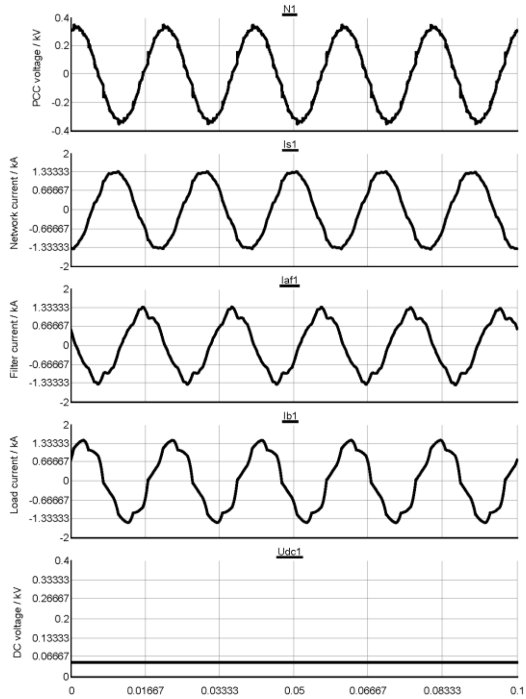

Fig. 9: Series HAPF simulated waveforms – voltage at HAPF PCC, supply (system) current, HAPF current, load current and voltage at the dc side of the converter.

in Fig. 8. Due to the transparency, only waveforms for one phase (L1) are shown. As can be seen, both the system current and the PCC voltage waveforms are nearly sinusoidal. The THD of the network current is less than 3 % and there is almost no distortion of the supply voltage due to switching of the IGBTs.

Fig. 10 shows simulation results of the series HAPF, with the same load conditions as in Fig. 8. The THD level of the supply current is above 5 % and also the distortion of the supply voltage is higher than with parallel HAPF. It is also important to note, that active part of the series HAPF has to withstand full nominal fundamental current.

CONCLUSION

In this paper a novel parallel hybrid active filter has been presented and compared with most common series hybrid filter. Since the rated power of the parallel active filter is almost three times lower than rated power of the series filter, the parallel filter presents viable and effective solution to reactive power compensation and harmonics elimination.

The performance of both hybrid filters was evaluated with simulations on RTDS. It has been shown that the parallel HAPF outperforms the series topology in filtering of harmonics.

REFERENCES

[1] R. C. Dougan, H. W. Beaty, *Electrical Power Systems Quality*, McGraw-Hill, 2002.

[2] J. C. Das, "Passive Filters - Potentialities and Limitations," *IEEE Trans. on Industry Applications*, vol. 40, no. 1, Jan./Feb. 2004.

[3] Hirofumi Akagi, "Trends in Active Power Line Conditioners", *IEEE Transactions on Power Electronics*, vol. 9, no. 3, 1994.

[4] J. H. Sung, S. Park, K. Nam, New Hybrid Parallel Active Filter Configuration Minimizing Active Filter Size, *IEE Proceedings Electric Power Applications*, March 2006, pp. 93.

[5] S. Senini and P. J. Wolfs, Hybrid Active Filter for Harmonically Unbalanced Three Phase Three Wire Railway Traction Loads, *IEEE Transactions on Power Electronics, vol. 15*, issue 4, 2000, pp. 702 – 710.

[6] L. Herman, I. Papič, "Design and Analysis of a State-Feedback-Controlled Hybrid Active Power Filter", *Special Issue on Power Quality in Smart Grids of International Review of Electrical Engineering*, Vol. 6, No. 6, November 2011.

[7] R. Teodorescu, F. Blaabjerg, M. Liserre, P.C. Loh, "Proportional-resonant controllers and filters for grid-connected voltage-source converters," *IEE Proceedings Electr. Power Applications*, Vol. 153, No. 5, Sept. 2006.

[8] C. Lascu, L. Asiminoaei, I. Boldea, F. Blaabjerg, "High Performance Current Controller for Selective Harmonic Compensation in Active Power Filters," *IEEE Transactions on Power Electronics*, Vol. 22, No. 5, Sept. 2007.

[9] H. Fujita, H. Akagi, "A practical approach to harmonic compensation in power systems series connection of passive and active filters," *IEEE Transactions on Industry Applications*, Vol. 27, Nov.-Dec. 1991.

[10] S. Bhattacharya, Po-Tai Cheng, D. M. Divan, "Hybrid Solutions for Improving Passive Filter Performance in High Power Applications," *IEEE Transactions on Industry Applications*, vol.33, no. 3, May-June 1997.

[11] S. Senini and P. J. Wolfs, Analysis and Comparison of new and Existing Hybrid Filter Topologies for Current Harmonic Removal, *Australasian Universities Power Engineering Conference*, Darwin, Australia, Sept. 27-30, 1999, pp. 227 – 232.